Seasonal Variability in the Intermediate Waters of the Eastern North Atlantic[1]

N. A. BRAY[2]

Woods Hole Oceanographic Institution, Woods Hole, MA 02543

(Manuscript received 31 December 1980, in final form 10 May 1982)

ABSTRACT

Observational evidence of seasonal variability below the main thermocline in the eastern North Atlantic is described, and a theoretical model of oceanic response to seasonally varying wind stress forcing is constructed to assist in the interpretation of the observations. The observations are historical conductivity-temperature-depth data from the Bay of Biscay region (2–20°W, 42–52°N), a series of eleven cruises over the three years 1972 through 1974, spaced approximately three months apart. The analysis of the observations utilizes a new technique for identifying the adiabatically leveled density field corresponding to the observed density field. The distribution of salinity anomaly along the leveled surfaces is examined, as are the vertical displacements of observed density surfaces from the leveled reference surfaces. Seasonal variations in salinity anomaly and vertical displacement occur as westward propagating disturbances with zonal wavelength 390 (±50) km, phase at the eastern boundary of 71 (±30) days from 1 January, and maximum amplitudes of ±30 ppm and ±20 db, respectively.

The observations are consistent with the predictions of a model in which an ocean of variable stratification with a surface mixed layer and an eastern boundary is forced by seasonal changes in a sinusoidal wind stress pattern, when wind stress parameters calculated from the data of Bunker and Worthington (1976) are applied.

1. Introduction

Seasonal variations in the strength of the wind are comparable in magnitude to the mean wind over much of the world's ocean. Consequently, significant seasonal fluctuations in the wind-driven ocean circulation might be anticipated. The hypothesis explored in this paper is that the observed annual variations in wind stress curl over the North Atlantic, in combination with a meridional barrier at the eastern edge of the ocean, are capable of producing seasonal variability below the main thermocline of sufficient amplitude to be detected observationally in the eastern part of the basin. The observational evidence is taken from a three-year series of hydrographic cruises in the eastern North Atlantic. A theoretical model of the oceanic response to seasonal wind stress forcing is constructed using the observed oceanic parameters, and the model prediction is compared with the observed variability.

2. Background

There is little historical evidence for seasonal variability in the oceans below the surface layers. The reason for this is twofold: only recently have observations of sufficiently long duration been available, and, except at low latitudes, the expected annual signal is small compared to the signals of the energetic western boundary currents and mesoscale eddies. In the near-equatorial region where the baroclinic response time of the ocean is shorter than at higher latitudes, seasonal variability has been observed. White (1977) found evidence for propagation of long baroclinic Rossby waves in the main thermocline (depth about 200 m) of annual period in MBT (mechanical bathythermograph) data from the tropical North Pacific. From the phase information he inferred that the source of the waves was the eastern boundary. In a similar analysis White (1978) presented evidence from the mid-latitude North Pacific for seasonal fluctuations in the depth of the main thermocline. He demonstrated that the phase of those fluctuations matched the phase of the observed wind-stress curl. The observed amplitude was 5–10 times that expected from the theory of Veronis and Stommel (1956), who modeled the case of an unbounded ocean forced by a variable wind stress.

In the mid-latitude North Atlantic the main thermocline is well removed from any direct solar influence. In the western part of the basin there is an energetic mesoscale eddy field associated with the Gulf Stream system. In the topographically confined Florida Current, whose transport contributes significantly to the Gulf Stream, Niiler and Richardson (1973) cite evidence of seasonal fluctuations representing half the total variability of the current and about 10% of its total transport. Away from the Flor-

[1] Contribution No. 4845 from the Woods Hole Oceanographic Institution.

[2] Present affiliation: Desalination Systems Inc., 1240 Simpson Way, Escondido, CA 92025.

0022-3670/82/090972-12$07.00

ida Strait, however, no evidence for seasonal variability below the main thermocline has been cited in the western North Atlantic. The energetic eddy field associated with the Gulf Stream will tend to mask the relatively weak annual signal expected in the interior, necessitating long observational records to detect the signal unambiguously. Wunsch (1972) computed spectra of temperature and dynamic-height anomaly using the 13 years of *Panulirus* hydrographic data taken semi-monthly at a single location near Bermuda. He found a pronounced annual peak in temperature at 10 m depth, a less pronounced peak at 100 m and none at 800 m. He also found annual peaks in the dynamic height anomaly spectra, but all the energy at that frequency comes from depths shallower than 200 m. Thus, even in a very long single record in the western North Atlantic, the seasonal signal, if it exists, has not been extracted from the noise.

Nevertheless, the available meteorological observations in the North Atlantic indicate that there is a strong annual cycle to the wind stress curl, with large horizontal scales (Bunker and Worthington, 1976), so that some annual response in the ocean interior is expected. It is anticipated that the observation of that annual signal is most likely to be made in the eastern basin, away from the energetic Gulf Stream system.

Bryan and Ripa (1978) constructed a model of the oceanic response to large-scale continuous wind forcing at low frequencies, for the special case of a flat-bottomed ocean with depth-variable stratification and a single meridional barrier at the eastern edge. They applied their model to the mid-latitude North Pacific at frequencies corresponding to periods of 3 and 6 years, using an idealization of the observed wind stress, and appropriate oceanic parameters. They calculated the resultant scales of the dominant free modes and estimated the apparent vertical propagation for comparison with observational estimates of the vertical propagation of low-frequency temperature anomaly structures in the North Pacific. Bryan and Ripa did not calculate the amplitude of the response. Their approach is appropriate to the present work, and their model is discussed in Section 3.

The region of the eastern North Atlantic in which the data used in this work were collected has no major sub-surface current systems, with the possible exception of a weak (0.01–0.05 m s^{-1}) poleward eastern boundary current of 60–250 km width and undetermined depth range. Away from the coast the available direct current measurements indicate very low mean flows (~0.01 m s^{-1}) (Swallow *et al.*, 1977). There is no evidence for a strongly energetic eddy field as is found in the western basin, although isolated eddy-like features have been observed (Swallow, 1969; Gascard, 1980) with velocities of 0.10–0.20 m s^{-1} associated with the cyclonic flow, and some indication of slow westward drift, on the order of 0.02 m s^{-1}.

In this region, the water masses found between the main thermocline and roughly 2000 m are Mediterranean Outflow Water (MOW), which originates in the western Mediterranean Sea and is characterized by high salinity as a function of temperature compared to North Atlantic Deep Water and Labrador Sea Water, formed in the Labrador Basin and similarly characterized by low salinity. The interaction of these two water masses within the area studied results in strong mean lateral gradients of salinity anomaly (defined as the difference between the observed salinity and a reference salinity). Needler and Heath (1975) and Katz (1970) discussed these strong lateral gradients. In the present work strong isopycnal gradients are used to detect the dynamic signal that results from horizontal displacements of parcels tagged by an initial salinity anomaly condition.

In order to study the lateral distribution of any tracer (such as salinity anomaly) it is necessary to define the density surfaces to be used. Ideally what is sought are those level surfaces which are connected to the observed density field by adiabatic displacements at each depth. A computational technique developed by Bray and Fofonoff (1981) for determining these implicit adiabatically leveled surfaces is used in the analysis of the hydrographic data, so that all discussions of salinity anomaly refer to distributions along leveled steric surfaces. The reader is referred to Bray and Fofonoff (1981) and Bray (1980) for details of the leveling technique.

3. Model

Although this work is primarily observational in nature, it utilizes an analytical model to assist in interpreting the observations. The model is described here, and the observations are discussed, using the model framework, in the following two sections. The model, which follows that of Bryan and Ripa (1978) assumes that the forcing consists of a waveform that may be propagating eastward or westward, or standing, and whose wavelength, phase, amplitude and frequency are parameters. The forcing is assumed to act upon the ocean through a mixed layer of finite depth as a body force rather than a stress. The model ocean is continuously stratified with depth-variable buoyancy frequency N below a surface mixed layer; the Coriolis parameter is allowed to vary with latitude in the usual β-plane approximation. There is a meridional barrier at the eastern edge of the basin, and no bottom topography, friction or diffusion. The stratification, mixed-layer depth and total depth are parameters. The oceanic response to the forcing consists of two parts: a forced wave of wavelength and frequency corresponding to the atmospheric forcing, and a sum of free waves required to satisfy the con-

straint of no flow into the boundary. The free waves are Rossby waves with meridional wavenumber equal to that of the forced wave, and zonal wavenumber determined by the Rossby-wave dispersion relation. The wind forcing and oceanic parameters are determined from the observations in Section 4. The free response zonal scales are determined primarily by the stratification, which is well known from the observations. Once the dominant free wave scales have been established, the model can then predict phase and horizontal and vertical displacements.

The predicted horizontal displacements, acting on a tracer field with mean horizontal gradients, will deform the initial tracer field (reversibly, in the absence of friction and diffusion) so that the progress of the disturbance through the fluid is traced by the anomaly in horizontal structure. Using the observed mean gradients of salinity anomaly (ΔS), the model predicts the amplitude and phase of the signal in ΔS.

The linearized quasi-geostrophic potential-vorticity equation with forcing is the dynamical basis of the model:

$$\left.\begin{aligned} &\frac{\partial}{\partial t}\left[\nabla_H^2 p - \frac{\partial}{\partial z}\left(\frac{f^2}{N^2}\frac{\partial p}{\partial z}\right)\right] - \beta\frac{\partial p}{\partial x} \\ &\qquad = f\rho_0\left(\frac{\partial Y}{\partial x} - \frac{\partial X}{\partial y}\right) \\ &fv = \frac{1}{\rho_0}\frac{\partial p}{\partial x} \\ &-fu = \frac{1}{\rho_0}\frac{\partial p}{\partial y} \\ &\nabla_H^2 = \frac{\partial^2}{\partial x^2} + \frac{\partial^2}{\partial y^2} \end{aligned}\right\}, \quad (1)$$

with ρ_0 the constant background density and X and Y body forces that parameterize the wind stress and are constant through the mixed layer and vanish below.

The boundary conditions applied are

$$\left.\begin{aligned} &w = 0 \quad \text{at} \quad z = 0, -H \\ &w(-h) = \frac{\text{curl}\,\tau}{\rho_0 f} \\ &w, p \quad \text{continuous across} \quad z = -h \\ &u = 0 \quad \text{at} \quad x = 0 \end{aligned}\right\}. \quad (2)$$

Here u is the zonal geostrophic velocity, p the geostrophic streamfunction, w the vertical velocity, H and h the ocean depth and mixed layer depth, and τ is the wind stress. There is also a radiation condition at $x = -\infty$ which requires that only waves with westward group velocity be included in the solution.

Following Bryan and Ripa (1978), an exponential $N(z)$ is chosen and (1) is solved by separation into vertically standing and horizontally propagating modes:

$$p = \hat{p}_f(z)\cos(ly)\exp(ik_f x - iwt) + \sum_{n=0}^{\infty}\hat{p}_n(z)\cos(ly)\exp(ik_n x - iwt),$$

where subscript f denotes the forced wave and subscript n denotes the nth free mode, with $n = 0$ the barotropic mode. The forcing is assumed to be of the form

$$X, Y = [\hat{X}\sin(ly), \hat{Y}\cos(ly)]\exp(ik_f x - iwt).$$

The complete solution for p is described in detail by Bray (1980) and will not be reproduced here. The solution differs from that of Bryan and Ripa in the inclusion of a barotropic wave.

The dispersion relation for the free waves is

$$k_n = -\frac{\beta}{2\omega} \pm \tfrac{1}{2}[(\beta^2/\omega^2) - 4(\lambda_n^2 + l^2)]^{1/2},$$

with λ_n the eigenvalues of the vertical structure function $\hat{p}_n$. For the observed parameters, only k_0 and k_1 are real; the higher order modes are coastally trapped.

The model described above is simplified to make it analytically tractable. Friction, diffusion and bottom topography are ignored; the complex geometry of the coastline has not been incorporated; and a geostrophic boundary condition is imposed at the coast. The neglect of bottom topography is not serious, as most of the observations are from the area of the Biscay Abyssal Plain. The effects of friction and diffusion are readily estimated, assuming values of A_H, A_v and K_H of 10^2, 10^{-2} and 10^3 m^2 s^{-1}, respectively. The ratios of these terms to the time derivative term in the momentum equation are 3×10^{-3}, 2.5×10^{-2} and 2.5×10^{-1}; only the neglect of lateral diffusion will introduce an appreciable error into the model solution.

The coastline used in the model is a simple meridional barrier, which is a reasonable approximation to the eastern coast of the North Atlantic over a scale of 5000 km. Locally, however, the coastal geometry is more complicated; in the Bay of Biscay it will be noted that the eastern boundary (taken as the shelf break) lies at an angle of perhaps 45° west of north (Fig. 1). If the model assumed an angled barrier of infinite extent, then there is a critical angle for which all free baroclinic modes are coastally trapped (Philander, 1978). In the parameters used in this model, that critical angle is 30° west of north. However, the constraint of infinite extent is unrealistic, especially since the north-south extent of the angled boundary

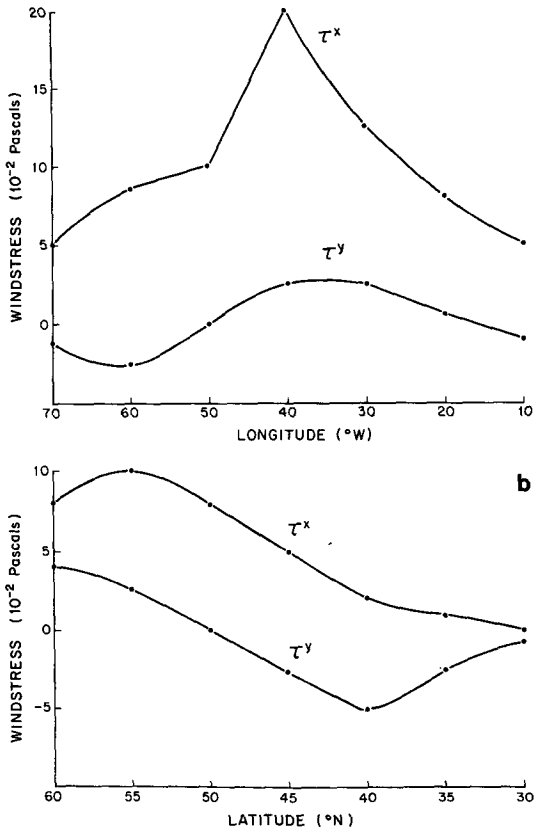

FIG. 1. Meridional sections (a) along 10°W and zonal sections (b) along 45°N of the annual average wind-stress components τ^x and τ^y. Values taken from Bunker and Worthington (1976).

is considerably less than the meridional scale of the forcing. In comparing model and observations x is taken to be the actual distance from the angled coast

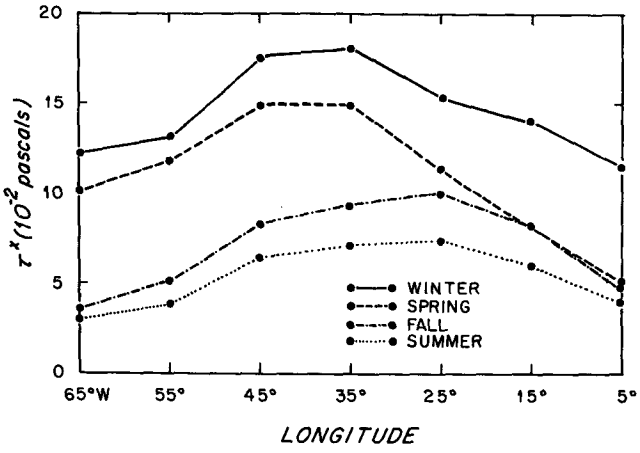

FIG. 2. Seasonal averages using all the Bunker and Worthington (1976) data (1948–72) of τ^x along 45°N, by 10° Marsden square.

TABLE 1. Description of *Phygas* cruises.

Phygas cruise	Day[1]	Depth[2] (m)	Instrument type	Number of stations[3]
22	124–135	1200	CTD	31 (15)
23	235–242	1250	CTD	70 (21)
24	294–307	1250	CTD	68 (24)
31	383–393	1750	CTD	58 (37)
32	480–492	1750	CTD	60 (38)
33	554–567	1700	CTD	44 (33)
34	627–641	1300	STD	76 (50)
41	780–794	1750	STD	54 (41)
42	908–920	1800	CTD	62 (48)
43	982–994	1750	STD	39 (39)
44	1076–1097	1750	CTD	47 (44)

[1] Covers the period during which stations within the small box (see Fig. 3) extending deeper than 1000 db were taken. Days are calculated from 1 January 1972.

[2] Maximum depth common to at least 10 stations, after regressions, for the restricted region.

[3] Total number of stations. In parentheses: number of stations within the restricted region (2–12°W, 43–48°N) deeper than 250 m.

(thereby a function of y), implying that the effect on the observations is simply a change in phase of the response.

In the model it is assumed that a geostrophic boundary condition may be applied at $x = 0$, i.e., that the Ekman contribution to the zonal velocity in the mixed layer is small compared to the geostrophic velocity there. For the parameters used in the model, those velocities are, in fact, of the same order of magnitude. The imbalance of mass flux in the mixed layer which results can only be eliminated by consideration of very thin side wall boundary layers (Pedlosky, 1979), a theoretical treatment beyond the scope of the present work.

4. Observations

a. *Wind stress*

There exists a comprehensive meteorological data set for the North Atlantic from 1948 to 1972 (Bunker and Worthington, 1976). Charts of the average annual wind stress over the North Atlantic were pre-

TABLE 2. Adiabatic leveling—regression parameters.

Depth range (db)	Interval between levels (db)	Regression interval (db)	Polynomial order
0, 200	50	250	6
250, 350	50	400	5
400, 450	50	500	5
500, 1100	50	450	5
1150, 2000	50	500	4

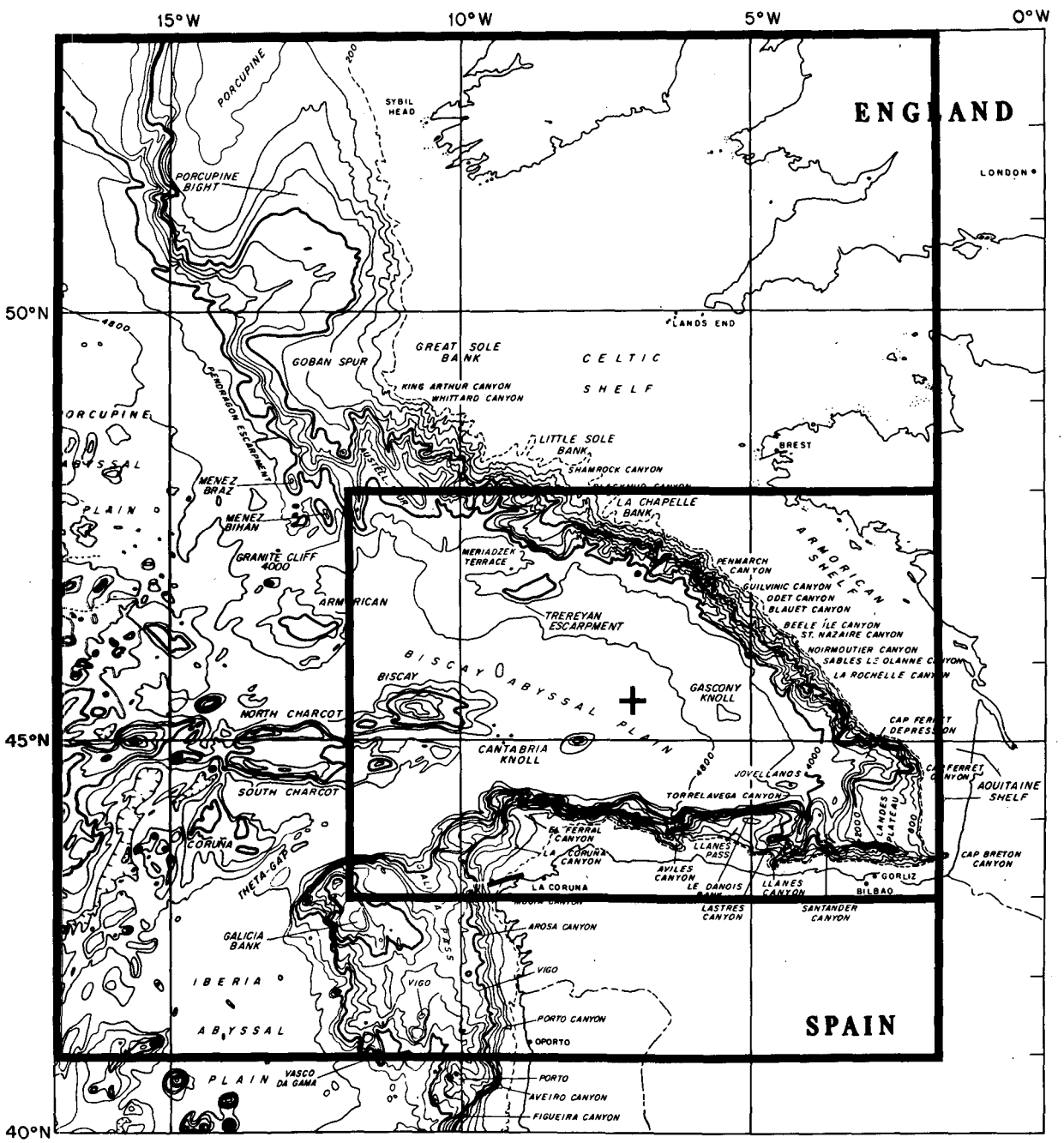

FIG. 3. General location of Bay of Biscay stations, showing bottom topography. The large box encloses all stations taken during the three-year period; the smaller box outlines area of greatest concentration of stations. The center of the smaller box, referred to in the text as the origin, is marked with a cross.

pared by Bunker and Worthington; to estimate the amplitudes and wavelengths of the annual wind-stress forcing appropriate to this problem, zonal and meridional sections of τ^x and τ^y (along 45°N and 10°W) were taken from those charts (see Fig. 1). The entire 25-year record of wind stress was examined for evidence of zonal phase propagation, with no conclusive results. There is some evidence that the zonal wind stress maximum shifts eastward in summer and fall relative to its position in winter and spring (Fig. 2). The forcing wavelengths used in the model were estimated from Fig. 1. The model results are not sen-

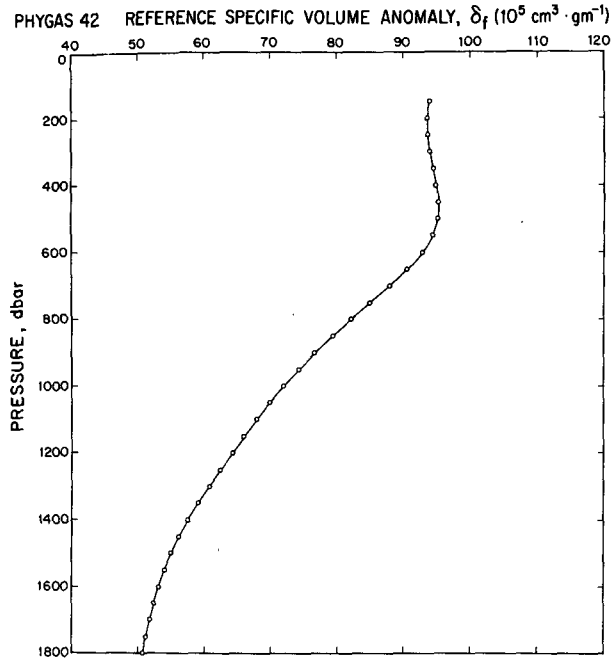

FIG. 4. Reference specific volume anomaly $\delta_f(p)$ for *Phygas* 42.

TABLE 3. Gradients of salinity anomaly at origin.

Depth (db)	Mean[1] S_x (S_{10}) (10^3‰) (km^{-1})	Mean[2] S_y (S_{01}) (10^3‰) (km^{-1})	Number of realizations[3] S_x	S_y
400	0.00 (0.03)	−0.05 (0.01)	11 (5)	(11)
600	−0.02 (0.04)	−0.09 (0.02)	11 (3)	(11)
800	−0.05 (0.16)	−0.24 (0.05)	11 (3)	(11)
1000	−0.11 (0.16)	−0.34 (0.08)	11 (5)	(11)
1200	−0.12 (0.21)	−0.42 (0.13)	11 (7)	(11)
1400	−0.10 (0.11)	−0.40 (0.10)	7 (1)	(7)
1600	+0.06 (0.16)	−0.28 (0.03)	7 (1)	(7)
1700	+0.08 (0.13)	−0.23 (0.04)	6 (1)	(6)

[1] Mean over all cruises of value of S_{10} at origin. In parentheses: standard deviation over all cruises.

[2] Mean over all cruises of value of S_{01} at origin. In parentheses: standard deviation over all cruises.

[3] In parentheses: S_x—number of realizations for which S_{10} is different from zero at the 95% confidence level; S_y—same as S_x, except for S_{01}.

sitive to the choice of forcing scales within reasonable limits. The forcing amplitudes were chosen such that the model salinity anomaly response amplitude was

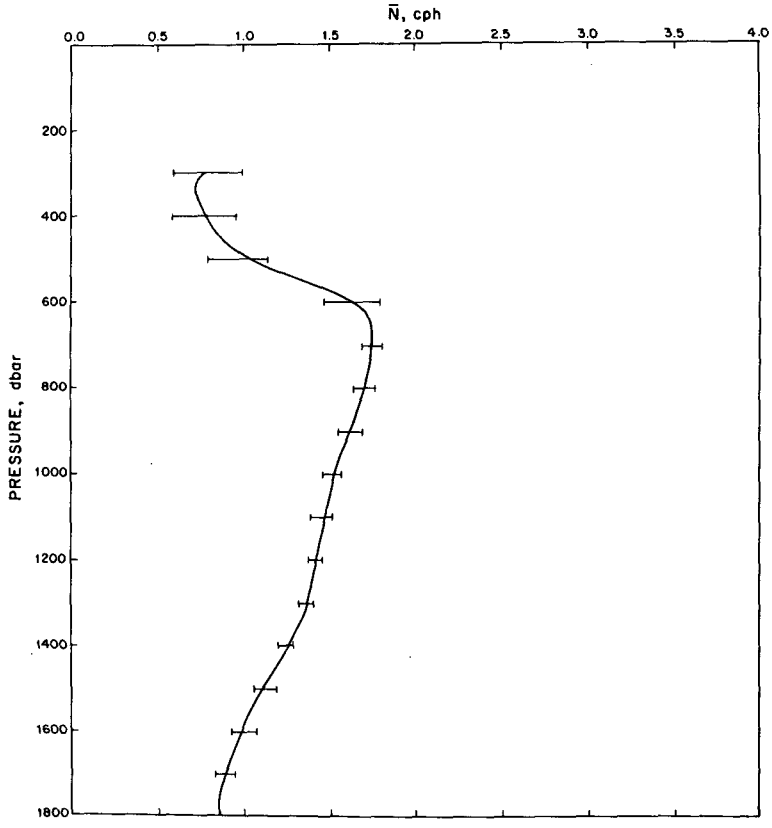

FIG. 5. Buoyancy frequency N, averaged over all stations, with the range of values from individual cruise averages given by horizontal lines at each depth.

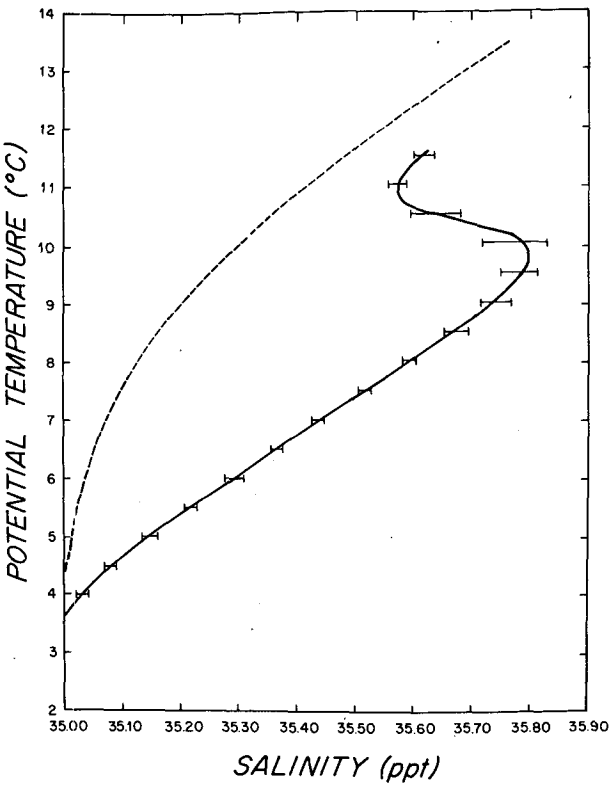

FIG. 6. Average θ vs S for all cruises (solid line). Dotted line is a cubic spline fit to θ vs S from Worthington and Metcalf (1961) and Iselin (1936) for the western North Atlantic.

approximately that given by the observations, with the ratio of τ^x/τ^y as given by the wind observations held constant. The wind stress amplitudes used in the model are 10×10^{-2} and -4×10^{-2} Pa for τ^x and τ^y, within a standard deviation of the 25-year regional mean values of 5×10^{-2} and 2×10^{-2} Pa. The phase of the seasonal cycle of wind stress was calculated by Firing (1978) for different longitude bands. At 38°N, between 30 and 40°W, he calculated that the maximum in wind stress occurred 55 days from 1 January.

b. *Hydrographic observations*

The hydrographic data used in this work are comprised of approximately 600 stations occupied by French investigators (Fruchaud, 1975; Fruchaud-Lapparra *et al.*, 1976,b) over a period of three years in the Bay of Biscay off the western coast of France. The stations were taken during eleven cruises spaced roughly three months apart; eight cruises used CTD (conductivity, temperature, depth) and three used STD (salinity, temperature, depth) instruments. The data were obtained through the U.S. National Oceanographic Data Center, in the format in which they were issued by the French organization Bureau National de Données Océaniques. The cruises are summarized in Table 1.

Most stations were occupied in a region bounded by 2 to 12°W and 43 to 48°N (see Fig. 3 and Table 1). For the purpose of comparison, only stations within those limits were used in the calculation of lateral fields. The bottom topography of that region (Fig. 3) is predominantly abyssal plain, although a sharp shelf break and steep continental slope mark the eastern, southern and angled northern boundaries. The simplicity of the topography does not extend much beyond the western boundary of the smaller region chosen for study.

The original version of the data is an uneven pressure series of approximately 1 db resolution. After making corrections for calibration errors, the acquisition group estimate the data to be accurate to ±0.01‰ in salinity, ±0.01°C in temperature and ±5 db in pressure. The original CTD data were converted to salinity, temperature and pressure by the author, using the algorithm from Fofonoff *et al.* (1974), and all the data were then pressure sorted and smoothed into even 10 db series.

As described briefly in Section 2, the data were analyzed using the adiabatic leveling technique developed by Bray and Fofonoff (1981). In that technique it is assumed that a given observed density field may be derived from a reference state in which density surfaces are level, i.e., correspond to pressure surfaces. The observed and reference states are connected by displacements which are adiabatic and isentropic (conserving heat and salt). Given the specific

TABLE 4. Typical error values for derived variables.

Variable	Measurement error	Vertical finestructure error	Horizontal fine-structure error
π	±5 db	±5 db	±7 db
δ_f	$\pm 0.5 \times 10^{-5}$ cm^3 g^{-1}	$\pm 0.2 \times 10^{-5}$ cm^3 g^{-1}	—
$S(\delta_f)$	±0.010‰	±0.010‰	±0.010‰
$\theta(\delta_f)$	±0.010°C	±0.010°C	±0.010°C

TABLE 5. Model parameters.

Parameter	Description	Value
h	mixed layer depth	400 m
H	total depth	5000 m
$2\pi/N_0$	buoyancy period at h	1.35×10^3 s
$1/\gamma$	e-folding depth for stratification	1300 m
$2\pi/k_f$	zonal wavelength of forcing	12000 km
$2\pi/l$	meridional wavelength of forcing	6000 km
$2\pi/\omega$	period	1 year
β	beta	1.6×10^{-11} (m s)$^{-1}$
f	Coriolis parameter	10^{-4} s^{-1}
τ^y	meridional wind stress	$10. \times 10^{-2}$ Pa
τ^x	zonal wind stress	$-4. \times 10^{-2}$ Pa

TABLE 6. Predicted wavelengths and phase speeds.

Mode	$2\pi/k$ (km)	ω/k (m s^{-1})
forced	12000.	0.381
barotropic mode	-4.1×10^5	−13.0
baroclinic modes		
1	−391.	−0.0125
>2	coastally trapped	

volume of the level surface, an implicit quantity which depends upon the three-dimensional density field, the distribution of any tracer along that surface may readily be calculated.

The leveling calculation is performed in two parts. First, all stations are fitted to polynomials such that pressure p and potential temperature θ (Fofonoff, 1977) are estimated as functions of specific volume anomaly δ. The regressions are performed over successive vertical intervals each centered about a chosen pressure surface p_f with specific volume and potential temperature referred to p_f. The intervals are permitted to overlap, and the regression order allowed to be a function of depth, but not of horizontal position. In the second half of the calculation the regression coefficients for pressure are averaged horizontally for each p_f, and, subject to the constraint that mass be conserved in the process of leveling, the equation for p_f as a polynomial function of the reference specific-volume anomaly δ_f is inverted to obtain δ_f. The variable parameters used in the initial regressions [$p(\delta)$, $\theta(\delta)$] are summarized in Table 2, with the values that were used in all eleven cruises.

As a background to the discussion of seasonal variability which is deferred to Section 5, a description of the time-mean fields in the region 2 to 12°W, 43 to 48°N is presented here. The vertical structure of the reference steric field δ_f changes very little with time. A typical plot of δ_f versus pressure is shown in Fig. 4. There is a deep, nearly mixed layer extending to about 400 m, with a weak main pycnocline below, and very little change in δ_f below the pycnocline. The average buoyancy frequency N profile in Fig. 5, which was constructed by averaging N horizontally at each pressure p_f for each cruise, and then averaging cruises, shows the same structure in a different perspective. There is a seasonal thermocline which is not plotted. The average θ–S relationship is plotted in Fig. 6, along with the standard θ–S curve of Worthington and Metcalf (1961) for the western North Atlantic for comparison (Armi and Bray, 1982). The dominance of MOW influence below the main thermocline is clear. Because the changes in salinity over the field are small compared to the salinity itself, and features of interest may be obscured, salinity anomaly (ΔS), defined as the difference between the observed salinity and that of the standard θ–S curve at the observed θ, was examined.

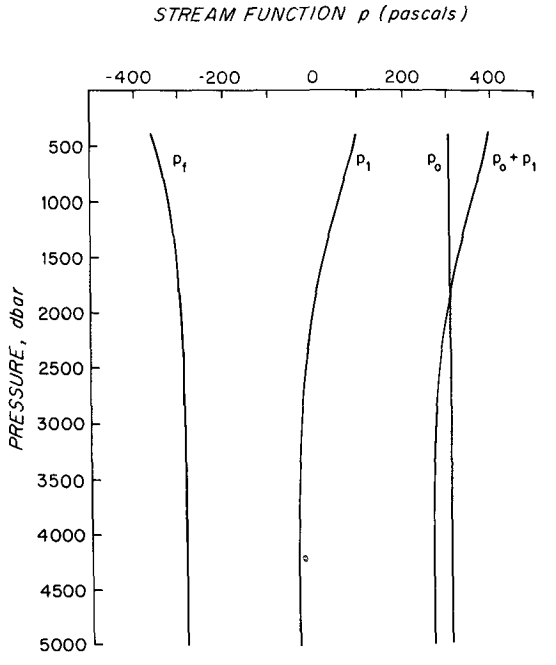

FIG. 7. Streamfunction $\hat{p}$ for eastward forced wave and corresponding barotropic and first baroclinic free waves.

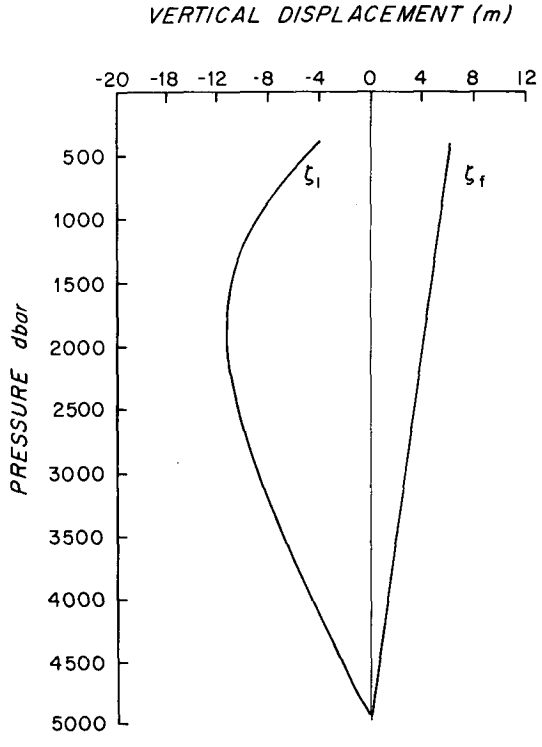

FIG. 8. Vertical displacements $\hat{\zeta}$ for eastward forced wave and corresponding first baroclinic wave.

The mean horizontal structure of the salinity anomaly field was determined using a least-squares linear regression in x (east) and y (north) distance from the origin at 45.5°N, 7°W (see Fig. 3):

$$\Delta S = \sum_{j=0}^{M} \sum_{i=0}^{M} \Delta S_{ij}(x - x_0)^i(y - y_0)^j,$$

with x_0 and y_0 the origin coordinates. These regressions were performed over adiabatically leveled steric surfaces corresponding to 400, 600, 800, 1000 and 1200 db for all cruises, and also over 1400, 1600, 1700 db for cruises with sufficiently deep data. The optimum number of terms in the regression was determined by examining the statistical confidence of the ratio of each coefficient ΔS_{ij} to its standard deviation. Four terms were identified at 95% confidence for most levels and cruises: ΔS_{00}, the average value; ΔS_{10}, the zonal (x) gradient; ΔS_{01}, the meridional (y) gradient; and ΔS_{20}, the zonal curvature or second derivative. The mean zonal and meridional gradients (using all stations) are listed in Table 3. Note that the gradients are evaluated at the origin. Vertical and horizontal finestructure errors can be estimated by examining the residuals of the corresponding regressions, as by Fofonoff and Bryden (1975). Those estimates are given in Table 4.

Similar regressions to those for ΔS were done using the vertical displacement π. A mean horizontal gradient in π would indicate a mean slope in the isopycnals; however, no discernable (i.e., 95% confidence) gradients in π were found.

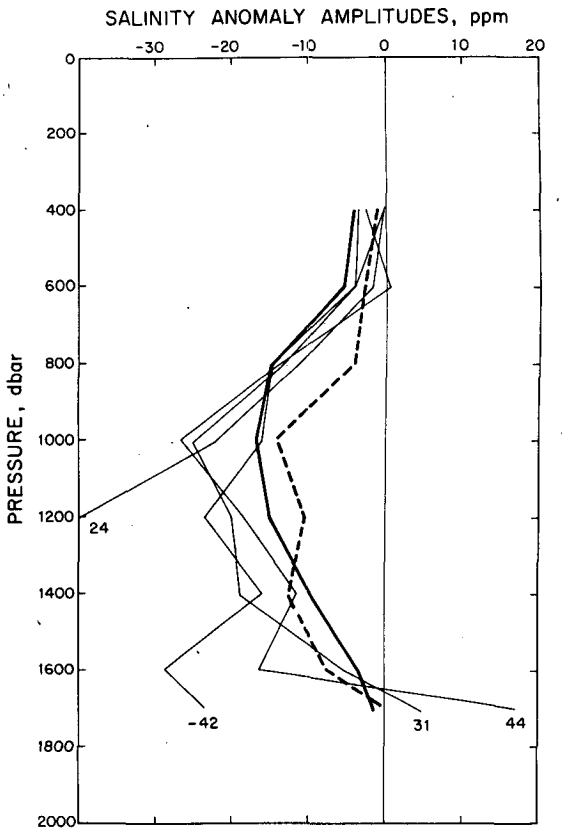

FIG. 10. Salinity anomaly amplitudes: heavy solid line is the model prediction, dashed line is the overall value (excluding cruises 42 and 43) and the remaining thin lines are cruises 24, 31, 44, and the negative of 42, as noted.

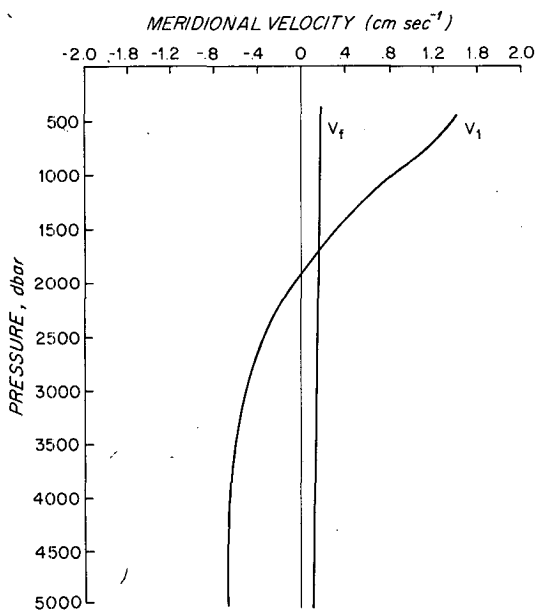

FIG. 9. Meridional velocity $\hat{v}$ for eastward forced wave and corresponding first baroclinic wave.

5. Comparison of model and observations

The parameters used in the calculation are listed in Table 5. The mixed-layer depth, total depth, and the stratification parameters are taken from the Bay of Biscay observations. The wavelengths and phase speeds of the forced barotropic and first baroclinic modes are given in Table 6. All of the baroclinic modes except the gravest are trapped within 20 km of the coast. The first baroclinic wave has a wavelength of 391 km. The barotropic wave is much longer than the basin and therefore has negligible displacements. Since the horizontal structure of the annual wind stress is not well known, the eastward propagating wave was chosen as representative and the results that follow are for that case.

The streamfunctions $\hat{p}_f$, $\hat{p}_0$, $\hat{p}_1$ are plotted in Fig. 7, illustrating the relative amplitudes of the barotropic and baroclinic components.

Displacement amplitudes ζ as a function of depth were calculated as

$$\frac{d\zeta}{dt} = \hat{w}(z)$$

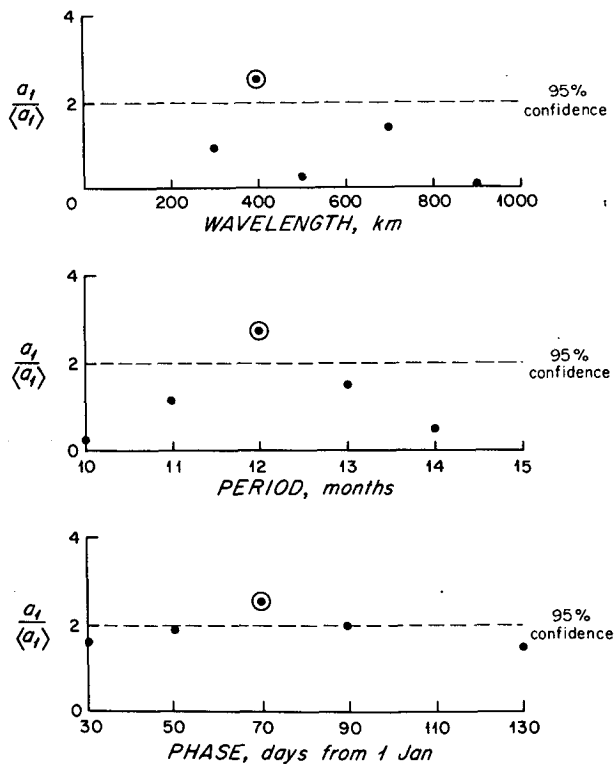

FIG. 11. Ratio of the least-squares computed salinity anomaly amplitude a_s to its standard deviation at 1000 db for ranges of wavelength, period and phase. Chosen parameters are circled.

or

$$\hat{\zeta} = \frac{-\hat{w}}{i\omega},$$

and are plotted in Fig. 8 for both the forced and the first free modes; ζ_f and ζ_1 are found to be of comparable amplitude. The meridional velocity amplitude

$$\hat{v} = k\hat{p}(z)$$

is plotted in Fig. 9, for the forced and first baroclinic modes. The meridional velocity of the barotropic mode is two orders of magnitude smaller than that of the forced mode, and is not pictured.

Since the free wave zonal velocity is much smaller than the meridional velocity, the salt conservation equation with no diffusion is approximately

$$\frac{\partial S}{\partial t} + v(x)\frac{\partial S}{\partial y} \approx 0.$$

Using the observed values of S_y from the Bay of Biscay data (Table 4), one may obtain an estimate of the salinity anomaly variation amplitude:

$$\Delta\hat{S} = -(S_y)_{\text{obs}}\frac{\hat{v}(z)}{i\omega},$$

which is plotted in Fig. 10 for those levels where $(S_y)_{\text{obs}}$ is available.

The model predicts westward propagating free disturbances of dominant wavelength 391 km, frequency 1 cycle per year (cpy) and phase corresponding to a maximum at 55 days from 1 January at the coast based upon the meteorological data. After the steady horizontal structure was removed, the residual salinity anomalies were fitted to

$$\Delta S = a_1 \sin(k_1 x - \omega t) + a_2 \cos(k_1 x - \omega t),$$

with $k_1 = (2\pi/391)$ km^{-1}, $\omega = (2\pi/365)$ days^{-1}, $a_1 = -a_s \sin\phi$, $a_2 = a_s \cos\phi$. ϕ is the phase at the eastern boundary and x is measured as actual horizontal distance from the 600 m isobath along the eastern boundary. The regression was done using all cruises at each level, and separately by cruise. In order to determine the amplitudes with statistical confidence greater than 90%, the best estimate of phase was used for ϕ, and the amplitude alone was fitted, with fixed phase. The best estimate of ϕ from the oceanographic observations corresponds to a maximum at 71 days from 1 January at the 600 m isobath. The estimated

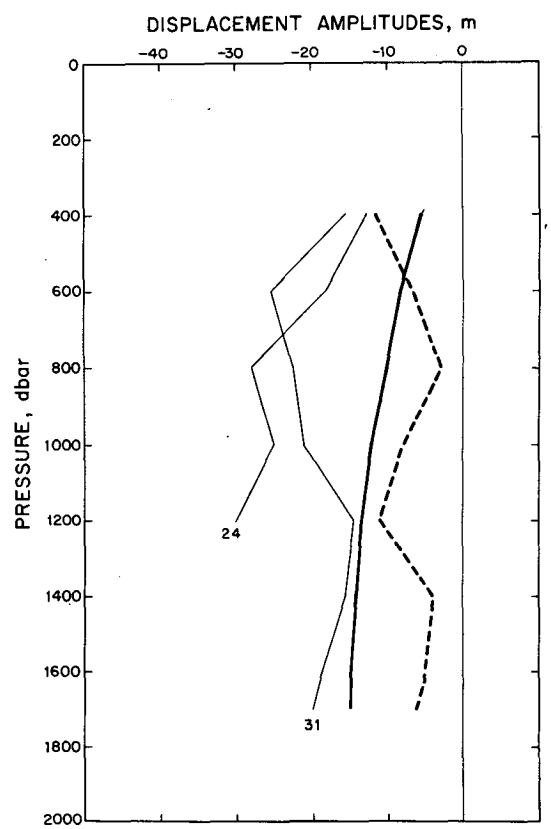

FIG. 12. Displacement amplitudes: heavy solid line is the model prediction, dashed line is the overall value (excluding cruises 42 and 43) and the thin lines are cruises 31 and 24.

error in the phase determination is ±0.3 rad (20 days), so that the calculated phase agrees with that of Firing (1978) within the errors of phase determination. The overall amplitude a_s as a function of z is plotted in Fig. 10, along with the amplitudes for cruises that show strong signals, and the model prediction for an eastward forced wave. Most of the variance in a_s is found in four cruises: *Phygas* 23, 31, 43, 44; the others contribute very little signal. The lack of signal may be due in part to insufficient sampling, as there are significantly fewer stations in those cruises (see Table 1). For *Phygas* 42 the amplitude a_s is positive, although it is plotted as $-a_s$ in Fig. 10. Negative amplitude occurs in the model only if the windstress curl is negative. Although this is not generally the case, negative curl represents less than two standard deviations from the mean. The vertical structure is similar in the four cruises with large signals, and compares very well with the model prediction.

In order to determine how sensitive the regression fit is to the chosen parameters k, ω and ϕ, tests were run using a range of values for each parameter, holding the other two at their chosen values. The ranges covered were

$2\pi/k$ (391 km):	300 to 900 km, steps of 100 and 200 km
$2\pi/\omega$ (12 months):	10 to 14 months, steps of 1 month
$\phi \cdot 365/2\pi$ (71 days):	50 to 130 days, steps of 20 days.

In all cases the ratio of the amplitude to its regression standard deviation was a maximum for the chosen parameters, and, with the exception of ϕ corresponding to 50–90 days, none other than the one with the three chosen parameters was significant at the 95% confidence level (see Fig. 11). The estimated error in the determination of ϕ given above is taken from these results.

A similar analysis was carried out for the displacement field, although there were no identifiable mean horizontal gradients to be removed. The observed displacement amplitudes $a_\pi(z)$ are plotted in Fig. 12 along with the model prediction and values for *Phygas* 31 and 24 which showed the most consistent single cruise results.

6. Conclusion

A seasonal signal in both horizontal and vertical displacement below the main thermocline in the eastern North Atlantic has been determined from observations that span a three-year period and an area of 500 km by 800 km. The signal is identifiable as a waveform with zonal wavelength 390 km and phase at the eastern boundary of 70 days from 1 January. The observed signal may be interpreted as resulting from eastern boundary reflection of a seasonally wind-forced, large-scale Rossby wave. The reflected first baroclinic mode dominates the seasonal signal in horizontal displacement, evidenced observationally by a strong signal in meridional velocity and hence in salinity anomaly. The forced wave and reflected first baroclinic mode have vertical displacements of comparable amplitude, resulting in a less clear but still discernable observation of seasonal signal in vertical displacement. The observed amplitude of the signal is O(25 ppm) in salinity anomaly and O(20 m) in vertical displacement.

Acknowledgments. Nick Fofonoff provided valuable advice and guidance during the course of this work. Discussions with Glenn Flierl contributed to the theoretical work presented here. William Schmitz, Harry Bryden and both reviewers contributed useful criticism regarding the manuscript. This work was supported by the Office of Naval Research under Contract N00014-76-C-197, NR 083-400.

REFERENCES

Armi, L., and N. A. Bray, 1982: A standard analytic curve of potential temperature versus salinity for the western North Atlantic. *J. Phys. Oceanogr.*, **12**, 384–387.

Bray, N. A., 1980: Seasonal variability in the intermediate waters of the eastern North Atlantic. Ph.D. thesis, MIT and WHOI Joint Program in Oceanography, 165 pp.

——, and N. P. Fofonoff, 1981: Available potential energy for MODE eddies. *J. Phys. Oceanogr.*, **11**, 30–47.

Bryan, K., and P. Ripa, 1978: The vertical structure of North Pacific temperature anomalies. *J. Geophys. Res.*, **83**, 2419–2429.

Bunker, A. F., and L. V. Worthington, 1976: Energy exchange charts of the North Atlantic Ocean. *Bull. Amer. Meteor. Soc.*, **57**, 670–678.

Firing, E., 1978: Seasonal oscillations in a mid-latitude ocean with barriers to deep flow. Ph.D. thesis, MIT and WHOI Joint Program in Oceanography.

Fofonoff, N. P., 1977: Computation of potential temperature of seawater for an arbitrary reference pressure. *Deep-Sea Res.*, **24**, 489–491.

——, and H. L. Bryden, 1975: Specific gravity and density of seawater at atmospheric pressure. *J. Mar. Res.* (Suppl.), **33**, 69–82.

——, S. P. Hayes and R. C. Millard, 1974: WHOI/Brown CTD microprofiler: methods of calibration and data handling. WHOI Tech. Rep. WHOI Ref. 74–89, 64 pp.

Fruchaud, B., 1975: Étude hydrologique et variations saisonnières dans le proche Atlantique en 1972. Rapp. Sci. Tech. CNEXO, No. 20, 44 pp.

Fruchaud-Lapparra, B., J. Le Floch, J. Y. Le Tareau and A. Tanguy, 1976a: Étude hydrologique et variations saisonnières dans le proche Atlantique en 1973. Rapp. Sci. Tech. CNEXO, No. 26, 111 pp.

——, ——, C. Le Roy, J. L. Le Tareau and F. Madelain, 1976b: Étude hydrologique et variations saisonnières dans le proche Atlantique en 1974. Rapp. Sci. Tech. CNEXO, No. 30, 108 pp.

Gascard, J., 1980: Mid ocean eddy in the northeastern Atlantic. *POLYMODE News*, No. 76, 9–10, Woods Hole Oceanographic Institution (unpublished manuscript).

Katz, E. J., 1970: Diffusion of the core of Mediterranean Water above the mid-Atlantic Ridge crest. *Deep-Sea Res.*, **17,** 611–625.

Needler, G. T., and R. A. Heath, 1975: Diffusion coefficients calculated from the Mediterranean salinity anomaly in the North Atlantic Ocean. *J. Phys. Oceanogr.*, **5,** 173–182.

Niiler, P. P., and W. S. Richardson, 1973: Seasonal variability of the Florida Current. *J. Mar. Res.*, **31,** 144–167.

Philander, S. G. H., 1978: Forced oceanic waves. *Rev. Geophys. Space Phys.*, **16,** 14–46.

Pedlosky, J., 1979: *Geophysical Fluid Dynamics.* Springer-Verlag, 624 pp.

Swallow, J. C., 1969: A deep eddy off Cape St. Vincent. *Deep-Sea Res.* (Suppl.), **16,** 285–295.

——, W. J. Gould and P. M. Saunders, 1977: Evidence for a poleward eastern boundary current in the North Atlantic Ocean. International Council for the Exploration of the Sea, Contribution to Statutory Meeting CM 1977/C:32 (unpublished manuscript).

Veronis, G., and H. Stommel, 1956: The action of variable wind stresses on a stratified ocean. *J. Mar. Res.*, **15,** 43–75.

White, W. B., 1977: Annual forcing of baroclinic long waves in the tropical North Pacific Ocean. *J. Phys. Oceanogr.*, **7,** 50–61.

——, 1978: A wind-driven model experiment of the seasonal cycle of the main thermocline in the interior mid-latitude North Pacific. *J. Phys. Oceanogr.*, **8,** 818–824.

Worthington, L. V., and W. G. Metcalf, 1961: The relationship between potential temperature and salinity in deep Atlantic water. *Rapp. P. V. Conseil Perm. Exp. Mer*, Vol. 149, 122–128.

Wunsch, C., 1972: Bermuda sea level in relation to tides, weather and baroclinic fluctuations. *Rev. Geophys. Space Phys.*, **10,** 1–49.